THE JOURNAL OF BIOLOGICAL CHEMISTRY
Vol. 278, No. 37, Issue of September 12, pp. 35687–35692, 2003
Printed in U.S.A.

Characterization of the Catalase-Peroxidase KatG from *Burkholderia pseudomallei* by Mass Spectrometry*

Received for publication, April 17, 2003, and in revised form, June 26, 2003
Published, JBC Papers in Press, June 29, 2003, DOI 10.1074/jbc.M304053200

Lynda J. Donald‡, Oleg V. Krokhin§, Harry W. Duckworth‡, Benjamin Wiseman¶, Taweewat Deemagarn¶, Rahul Singh¶, Jack Switala¶, Xavi Carpena‖, Ignacio Fita‖, and Peter C. Loewen¶

From the Departments of ‡Chemistry, §Physics, and ¶Microbiology, University of Manitoba, Winnipeg, Manitoba R3T 2N2, Canada and ‖Institute de Biologíe Molecular de Barcelona, Consejo Superior de Investigacione Cientifícas, Jordi-Girona 18-26, 08034 Barcelona, Spain

The electron density maps of the catalase-peroxidase from *Burkholderia pseudomallei* (BpKatG) presented two unusual covalent modifications. A covalent structure linked the active site Trp^{111} with Tyr^{238} and Tyr^{238} with Met^{264}, and the heme was modified, likely by a perhydroxy group added to the vinyl group on ring I. Mass spectrometry analysis of tryptic digests of BpKatG revealed a cluster of ions at *m/z* 6585, consistent with the fusion of three peptides through Trp^{111}, Tyr^{238}, and Met^{264}, and a cluster at *m/z* ~4525, consistent with the fusion of two peptides linked through Trp^{111} and Tyr^{238}. MS/MS analysis of the major ions at *m/z* 4524 and 4540 confirmed the expected sequence and suggested that the multiple ions in the cluster were the result of multiple oxidation events and transfer of CH_3-S to the tyrosine. Neither cluster of ions at *m/z* 4525 or 6585 was present in the spectrum of a tryptic digest of the W111F variant of BpKatG. The spectrum of the tryptic digest of native BpKatG also contained a major ion for a peptide in which Met^{264} had been converted to homoserine, consistent with the covalent bond between Tyr^{238} and Met^{264} being susceptible to hydrolysis, including the loss of the CH_3-S from the methionine. Analysis of the tryptic digests of hydroperoxidase I (KatG) from *Escherichia coli* provided direct evidence for the covalent linkage between Trp^{105} and Tyr^{226} and indirect evidence for a covalent linkage between Tyr^{226} and Met^{252}. Tryptic peptide analysis and N-terminal sequencing revealed that the N-terminal residue of BpKatG is Ser^{22}.

The heme-containing catalase-peroxidases are bifunctional enzymes that degrade hydrogen peroxide either as a catalase ($2H_2O_2 \rightarrow 2H_2O + O_2$) or as a peroxidase ($H_2O_2 + 2AH \rightarrow 2H_2O + 2A^{\cdot}$). The catalatic reaction, with a more rapid turnover rate, dominates over the peroxidatic reaction, and the *in vivo* peroxidatic substrate remains unidentified, suggesting that the main role of the enzyme is the removal of H_2O_2, preventing the formation of highly reactive and damaging breakdown products of H_2O_2. However, the enzyme has a close sequence resemblance to plant peroxidases (1, 2), and it remains a possibility that the peroxidatic reaction has a metabolic significance outside of degrading H_2O_2. Indeed, it is clear that the catalatic function evolved as an adaptation of the peroxidatic function because the simple change of a tryptophan to a phenylalanine in the distal heme pocket reduces catalatic activity by 1000-fold (of *Escherichia coli* HPI) and increases peroxidatic activity by 3-fold (3–5). Furthermore, the core structures of both the N- and C-terminal domains of the catalase-peroxidases from *Haloarcula marismortui* and *Burkholderia pseudomallei* closely resemble the structure of plant peroxidases (6, 7). Finally, the conversion of isoniazid into its active antitubercular form by KatG of *Mycobacterium tuberculosis* is clearly a result of the peroxidatic reaction using isonicotinic acid hydrazide (INH)[1] as a substrate that must mimic the actual *in vivo* substrate.

The structures of the catalase-peroxidases from *H. marismortui* and *B. pseudomallei* have been reported (6, 7) and have revealed several features that are, so far, unique to this class of enzyme. Present in both structures is an unusual adduct or covalent linkage among the side chains of a tryptophan, a tyrosine, and a methionine (see Fig. 1). The likely mechanistic significance of the covalent structure is enhanced by the fact that the tryptophan lies in the active site and is essential for catalatic activity. A second feature, evident only in the structure of BpKatG, is a modification to the heme, likely a hydroperoxide group added to ring I of the heme in close proximity to the Trp-Tyr-Met adduct. This paper presents mass spectrometry evidence supportive of the existence of the Trp-Tyr-Met adduct originally deduced from the electron density maps of HmCPx and BpKatG (6, 7).

EXPERIMENTAL PROCEDURES

Materials—Standard chemicals and biochemicals were obtained from Sigma. Restriction endonucleases, polynucleotide kinase, DNA ligase, and the Klenow fragment of DNA polymerase were obtained from Invitrogen.

Strains and Plasmids—The plasmid pBG306 encoding BpKatG (8) and the plasmids pAH8 and pW105F encoding KatG (HPI) and its W105F variant from *E. coli* (3) were transformed into strain UM262 *pro leu rpsL hsdM hsdR endI lacY katG2 katE12*::Tn*10 recA* (8) for expression of the *katG* constructs and isolation of the mutant KatG proteins. Phagemids pKS^+ and pKS^- from Stratagene Cloning Systems were used for mutagenesis, sequencing, and cloning. *E. coli* strains NM522 (*supE thi*) (*lac-proAB*) *hsd-5* [F′ *proAB lacI*^{q} *lacZ*)*15*]) (9), JM109 (*recA1 supE44 endA1 hsdR17 gyrA96 relA1 thi*) (*lac-proAB*) (10), and CJ236

* This work was supported by Grants BIO099-0865 and BIO2002-04419 from Direccion General de Investigacion Ciencia y Technologia (to I. F.) and Grant OGP9600 from the Natural Sciences and Engineering Research Council of Canada (to P. C. L.). The costs of publication of this article were defrayed in part by the payment of page charges. This article must therefore be hereby marked "*advertisement*" in accordance with 18 U.S.C. Section 1734 solely to indicate this fact.

** To whom correspondence should be addressed: Dept. of Microbiology, University of Manitoba, Winnipeg, MB R3T 2N2, Canada. Tel.: 204-474-8334; Fax: 204-474-7603; E-mail: peter_loewen@umanitoba.ca.

[1] The abbreviations used are: INH, isonicotinic acid hydrazide; MALDI, matrix-assisted laser desorption ionization; MS, mass spectrometry; HPLC, high pressure liquid chromatography; HPI, hydroperoxidase I.

TABLE I
Characterization of BpKatG and its variants

Variant	Catalase	Peroxidase
	units/mg	*units/mg*
BpKatG	1010	1.1
R108K	90	0.55
W111F	1.3	0.33
M264L	2.4	1.3

(*dut-1 ung-1 thi-1 relA1*/pCJ105 F′) (11) were used as hosts for the plasmids and for generation of single-stranded phage DNA using helper phage R408.

Oligonucleotide-directed Mutagenesis—The oligonucleotides CTGTTCATC**AAA**ATGGCATGG (AAA encoding Lys in place of Arg^{108}), CGCATGGCA**TTT**CACAGCGCG (TTT encoding Phe in place of Trp^{111}), and TTCGCGCGC**CTG**GCGATGAAC (CTG encoding Leu in place of Met^{264}) were purchased from Invitrogen. They were used to mutagenize a 600-bp fragment from pBG306 generated by *Kpn*I-*Cla*I restriction following the Kunkel procedure (11), which was subsequently reincorporated into pBG306 to generate the mutagenized *katG* gene. Sequence confirmation of all sequences was by the Sanger method (12) on double-stranded plasmid DNA generated in JM109. Subsequent expression and purification were carried out as described previously (3, 8). The catalase- and peroxidase-specific activities of the variants compared with the native BpKatG are summarized in Table I.

Catalase, Peroxidase, Protein, and Spectral Determination—Catalase activity was determined by the method of Rørth and Jensen (13) in a Gilson oxygraph equipped with a Clark electrode. One unit of catalase is defined as the amount that decomposes 1 μmol of H_2O_2 in 1 min in a 60 mM H_2O_2 solution at pH 7.0 at 37 °C. Protein was estimated according to the methods outlined by Layne (14). Peroxidase activity was determined by the method of Smith *et al.* (15). One unit of peroxidase is defined as the amount that decomposes 1 μmol of 3-ethylbenzothiazolinesulfonic acid in 1 min at 20 °C. Absorption spectra were obtained using a Milton Roy MR3000 spectrophotometer. The samples were dissolved in 50 mM potassium phosphate, pH 7.0.

N-terminal Sequencing—The N-terminal sequence was determined by the Proteomics facility at the Institut de Biotecnologia i Biomedicina.

Mass Spectrometry Analysis—For mass spectrometry, protein was dialyzed into 5 mM ammonium acetate. The intact proteins were analyzed by electrospray ionization in an orthogonal time-of-flight mass spectrometer (16, 17). The declustering voltage was varied to assess the stability of the protein-heme complex. Digests of the proteins were prepared using tosylphenylalanyl chloromethyl ketone-treated trypsin and analyzed on the Manitoba/Sciex prototype MALDI QqTOF instrument (18). Initial analysis was done with equal volumes (0.5 μl) of digested protein and 2,5-dihydroxybenzoic acid (160 mg/ml in water: acetonitrile 3:1, 2% formic acid) spotted onto a custom target. Further separation was achieved by microliquid chromatography on the Agilent 1100 Series system. The samples (5 μl) were injected onto a 100-μm I.D. × 150-mm column (Vydac 218 TP C18, 5 μm) and eluted with a linear gradient of 1–80% acetonitrile (0.1% trifluoroacetic acid). Column effluent (4 μl/min) was collected at 1-min intervals by hand. Under the conditions used, the vast majority of tryptic fragments were eluted in 40 min. These were spotted onto the target as described above.

RESULTS

MS Characterization of the Trp-Tyr-Met Adduct in BpKatG—The existence of a covalent structure linking the side chains of Trp^{111}, Tyr^{238}, and Met^{264} in BpKatG (Fig. 1) was originally deduced from the electron density maps derived from crystals of both HmCPx (6) and BpKatG (7). To confirm the existence of such an unusual structure, the peptide mixture generated by trypsin digestion of BpKatG was analyzed by mass spectrometry. Each of the key residues in the structure is located on a separate tryptic peptide fragment, and the absence of these fragments combined with the presence of larger fragments of appropriate mass would confirm the presence of the adduct (Fig. 2). Some of the peptides identified by MALDI mass spectrometry from both BpKatG and its W111F variant are listed in Table II. Significantly, the expected fragment at *m/z* 1179 (containing Trp^{111}) is completely absent from the BpKatG spectrum, but the equivalent ion in the spectrum of the W111F

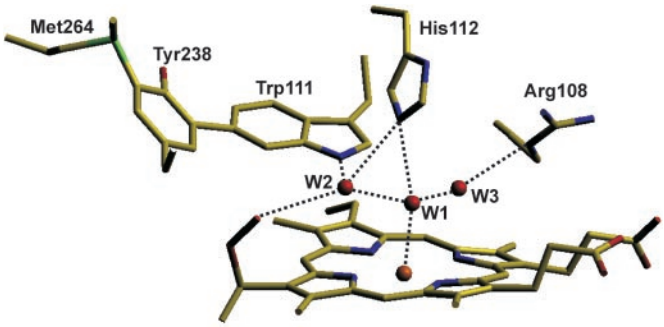

FIG. 1. **Schematic showing the key residues in the heme-containing active site of BpKatG.** The perhydroxy group on the vinyl group of ring I of the heme and the covalent bonds linking Trp^{111} to Tyr^{238} and Tyr^{238} to Met^{264} are indicated. The classic triad of active site residues on the distal side of the heme in peroxidases includes Arg^{108}, Trp^{111}, and His^{112}. The *dashed lines* indicate possible hydrogen bonds. The figure was prepared using SETOR (19).

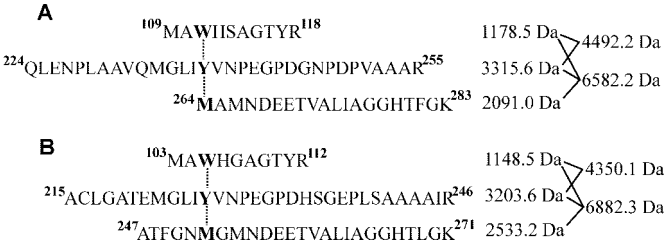

FIG. 2. **Sequences of the three peptides containing, respectively, Trp^{111}, Tyr^{238}, and Met^{264} that are covalently linked in BpKatG (*A*) and Trp^{105}, Tyr^{226}, and Met^{252} in HPI (*B*).** The *dashed lines* indicate possible covalent links, and the sizes of the peptides are shown on the *right* along with the sizes of the peptides that would result from Trp-Tyr and Trp-Tyr-Met covalent linkages.

variant, shifted to *m/z* 1140 by the Trp to Phe replacement, is clearly evident. The ions at *m/z* 2092 (containing Met^{264}) and *m/z* 3316 (containing Tyr^{238}) are present in the spectra of both BpKatG and its W111F variant, although they are less prominent in the former spectrum. Furthermore, two additional clusters of ions are evident in the BpKatG spectrum that are not present in the W111F spectrum, near *m/z* 4525 and *m/z* 6585, very close to the sizes predicted for combined peptides in the Trp-Tyr and Trp-Tyr-Met adducts, respectively (Fig. 3). The large size of the ions of the triple adduct at *m/z* 6585 precluded further analysis by MS/MS. The cluster of ions corresponding to the double adduct at *m/z* 4525 (Fig. 3) contains a series of seven peaks separated by increments of ~16 Da beginning at *m/z* 4493, with two predominant ions at *m/z* 4524 and 4540. These ions were analyzed by MS/MS revealing a series of fragments consistent with the proposed structure (Fig. 3*C* and Table III), albeit with additions of 30–31 and 46–47 Da, respectively, in the ions at *m/z* 4524 and 4540. At least two explanations for the additional mass are possible. One explanation is that two (32 Da) or three (48 Da) oxygens are added along with the associated loss of 1 or 2 protons, and this is supported in part by the apparent oxidation of the indole ring of Trp^{111} evident in the electron density maps. The second explanation is that the hydrolysis of the Tyr-Met covalent bond (Fig. 4) results in the CH_3-S (46 Da or +47 Da less 1 proton) from the methionine being transferred to the tyrosine, *ortho* to the HO, in some fraction of the products. In fact, a mixture of overlapping ions containing multiple oxygens and the CH_3-S group is necessary to explain the presence of the seven or more ions in the cluster near *m/z* 4525 and the prevalence of larger ions.

The transfer of the CH_3-S to the Tyr is clear indirect evidence for the presence of a covalent linkage between Tyr^{238} and

TABLE II
Observed and expected monoisotopic [M + H$^+$] masses of selected ions from the tryptic digest of BpKatG and its W111F variant

Expected ion (*m/z*)	Observed in BpKatG	Observed in W111F	Residues	Sequence	Confirmed by MS/MS
1140.53	No	1140.53	109–118	MAFHSAGTYR	Yes
1179.54	No	No	109–118	MAWHSAGTYR	
1459.65	1459.65	1459.65	27–40	CPFHQAAGNGTSNR	Yes
2062.06	No	No	1–18	MPGSDAGPRRRGVHEQRR	
	2061.99	No	264–283	XAMNDEETVALIAGGHTFGK	Yes
2091.98	2091.99	2091.99	264–283	MAMNDEETVALIAGGHTFGK	Yes
3316.66	3316.62	3316.64	224–255	QLENPLAAVQMGLIYVNPEGPDGNPDPVAAAR	Yes
		3332.66	224–255	Oxidation of 224-255	Yes
4493.18	4493[a]	No		Trp-Tyr adduct of 109-118 and 224-255	No
	4509[a]	No		One oxidation of Trp-Tyr adduct	No
	4525[a]	No		Two oxidation of Trp-Tyr adduct	Yes
	4543[a]	No		Three oxidations and/or CH_3-S added to Trp-Tyr adduct	Yes
	No	4555[a]		Unknown	No
	4557[a]	No		Mixed ion of oxidized and modified Trp-Tyr adduct	No
	4573[a]	4573[a]		Mixed ion of oxidized and modified Trp-Tyr adduct	No
	4589[a]			Mixed ion of oxidized and modified Trp-Tyr adduct	No
6583.17	6585[a]	No		Trp-Tyr-Met adduct of 109-118, 224-255, and 264-283	No

[a] Average *m/z* of the cluster is presented. Difficulty in identifying the real monoisotopic ion in a mixture of ions precludes the accurate measurement of masses. The identification of oxidized forms of the fragments is complicated by the fact that every ion produces two daughter ions, from loss of water (−18) and loss of NH_3 (−17), giving rise to three overlapping series of ions differing by +16, −17, and −18. The situation is further complicated by the possibility that CH_3-S may also be present, producing a +46 series.

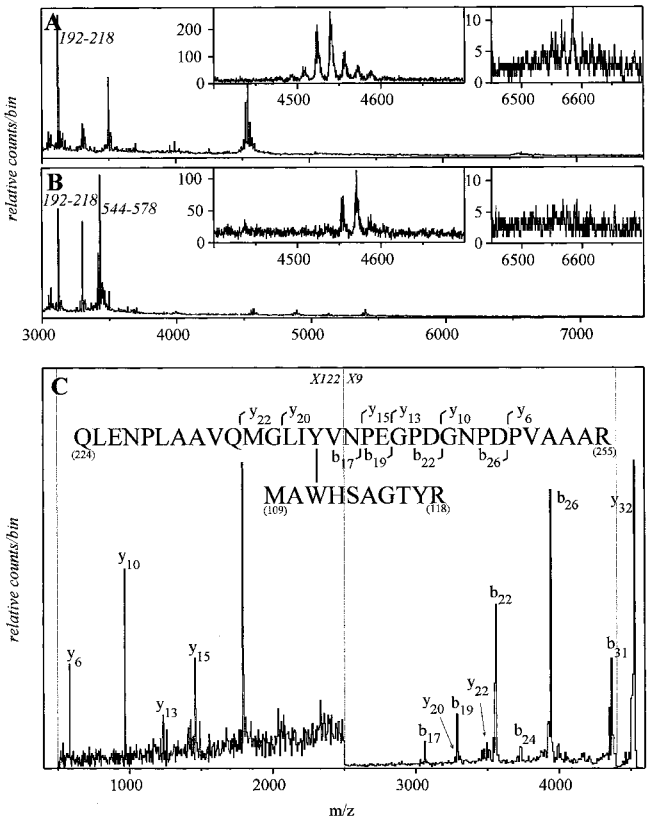

FIG. 3. **High *m/z* range MALDI spectra of comparable HPLC fractions from tryptic digests of native BpKatG and its W111F variant.** *A*, the spectrum of HPLC fraction 24 of the digest of native BpKatG contains a prominent cluster of ions at *m/z* ~4525 (expanded in the *inset*) formed by the covalent linkage between Trp^{111} and Tyr^{238}. A small cluster of ions is also evident at *m/z* 6585, consistent with the presence of the covalent bonds between Trp^{111} and Tyr^{238} and between Tyr^{238} and Met^{264}. *B*, the spectrum of HPLC fraction 29 of the digest of the W111F variant lacks the same ion cluster at *m/z* ~4525. The ions present in this region differ in size and are present at much lower amounts (see scale). *C*, partial MS/MS analysis of the ion at *m/z* 4524 from *A*. The location of the cleavage sites giving rise to the various ions are shown by a *vertical line* and ion designation above or below the sequence The ions y32, y22, y20, and y18 and all of the b series are 30–31 Da larger than expected from the sequence shown, whereas the y6 to y15 ions agree well with the expected sizes. The fragment sizes are summarized in Table III. The ion at *m/z* 1792 was not identified.

TABLE III
Comparison of expected and observed mono-isotopic M + H$^+$ masses of ions in the MS/MS spectrum of the ion at m/z 4524 shown in Fig. 3C and in the MS/MS spectrum of the ion at m/z 4540

N	Expected ion	*m/z* 4524		*m/z* 4540	
		Observed	Difference	Observed	Difference
y ions					
y32	4493.18	4524.15	30.97	4540.18	47.00
y29	4123.00			4169.69	46.69
y22	3429.62	3459.67	30.05	3474.81	45.19
y20	3241.56	3269.56	28.00		
y18	3015.39			3060.21	44.82
y15	1462.69	1462.64	0.05	1462.73	0.04
y13	1236.60	1236.57	0.03	1236.59	0.01
y10	967.50	967.48	0.02	967.49	0.01
y6	584.35	584.35	0.00	584.35	0.00
b ions					
b15				2863.90	45.51
b17	3031.50	3061.51	30.01	3077.45	45.95
b19	3257.59	3287.54	29.95	3303.61	46.02
b22	3526.70	3556.66	29.96	3572.73	46.03
b24	3697.76	3728.58	30.82	3743.66	45.90
b26	3909.84	3939.81	29.97	3955.81	45.97
b31	4319.07	4350.02	30.95	4366.06	46.99
b32	4475.17	4506.09	30.92	4522.18	47.01

Met^{264} that was broken during mass spectrometry analysis and suggests that the remainder of the cleaved methionine should be present in one of the ions. The expected ion for the Met^{264}-containing peptide at *m/z* 2092 is present in the spectra of both BpKatG and the W111F variant but is accompanied by an unexpected ion at *m/z* 2062 only in the BpKatG spectrum (Fig. 5, *A* and *B*). MS/MS analysis of the ions at *m/z* 2062 and 2092 (Fig. 5, *C* and *D*, and Table IV) reveals the common sequence *X*AMNDEETVALIAGGHTFGK, in which *X* has the correct mass for Met in the ion at *m/z* 2092 but has a mass 30 Da smaller in the ion at *m/z* 2062. For the fragmentation of the ion at *m/z* 2062, all of the b series ions, containing the N-terminal residue, are 30 Da smaller than the expected mass, whereas all of the y series ions, with the exception of y32, are in agreement with the expected *m/z* values (Table IV). Assigning *X* as homoserine, which would arise from hydrolysis of the Tyr-Met covalent bond (Fig. 4) and which has a mass 30 Da less than that of Met, explains the mass differential between the ions at *m/z* 2062 and *m/z* 2092. In addition, this represents further indirect evidence for the covalent link between Tyr^{238} and Met^{264}.

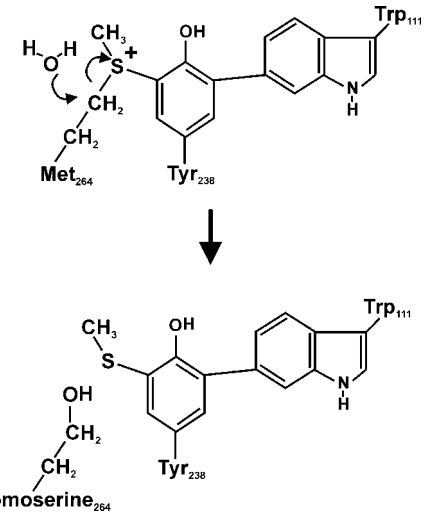

FIG. 4. **Possible pathway for hydrolytic cleavage of the covalent bond linking Tyr^{238} and Met^{264} generating homoserine from methionine.**

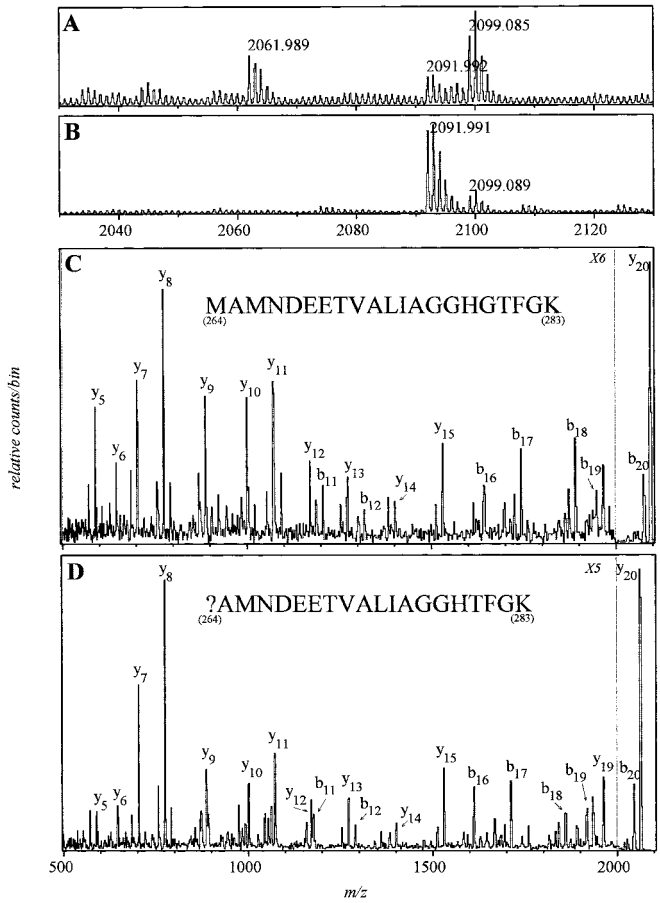

FIG. 5. **MALDI spectra at *m/z* ~2100 of the tryptic digest of native BpKatG (*A*) and of the W111F variant (*B*); MS/MS of the expected ion at *m/z* 2091.99 (*C*) and of the anomalous ion at *m/z* 2061.99 (*D*).** The locations of the cleavage sites giving rise to the various ions are shown by *vertical lines*, and the ion designation is above or below the sequence. The monoisotopic $M+H^+$ values for the ions in *C* and *D* are summarized in Table IV.

MS Characterization of the Trp-Tyr-Met Adduct in HPI—The presence of the covalent adduct in catalase-peroxidases from two such disparate sources as the archaebacterium *H. marismortui* and the Gram-negative bacterium *B. pseudomallei* suggested that it may be a feature common to all catalase-peroxidases. This was explored in an analysis of the tryptic digest of HPI (KatG) from *E. coli* and its W105F variant (Table V). All three of the fragments containing, respectively, Trp^{105} (*m/z* 1149), Met^{252} (*m/z* 2532), and Tyr^{226} (*m/z* 3206) are present, with their identities confirmed by MS/MS analysis. Although this suggests that the adduct may not be present in HPI, a cluster of ions, also separated by ~16 Da, is evident near *m/z* 4350 (Fig. 6*A*) in the digest of native HPI but not in the digest of the W105F variant (Fig. 6*B*). Analysis of the predominant ion by MS/MS reveals a fragmentation pattern consistent with the presence of the Trp-Tyr covalent structure (Fig. 6*C*). The location of the modifications, either from the addition of CH_3-S (+47 less one proton for +46) or oxidation (+48 for three oxygen atoms less 2 protons for +46), could be localized to the hybrid fragment bounded by ions y25 and y16 (Fig. 6*C* and Table VI). Unfortunately, ions at *m/z* 6885, indicative of the triple adduct, and *m/z* 2504, indicative of Met^{252} modified to homoserine, were not identified, making the only evidence for the Tyr-Met portion of the adduct in HPI the possible presence of CH_3-S in the ion at *m/z* 4351.

TABLE IV
Comparison of expected and observed mono-isotopic M + H$^+$ masses of ions in the MS/MS spectra shown in Fig. 5 (C and D)

N	Expected ion	Fig. 5*C*		Fig. 5*D*	
		Observed	Difference	Observed	Difference
y ions					
y20	2091.98	2091.98	0.00	2062.01	−29.97
y19	1960.94			1961.01	0.07
y15	1529.80	1529.84	0.04	1529.79	−0.01
y14	1400.75	1400.74	−0.01	1400.73	−0.02
y13	1271.71	1271.69	−0.02	1271.72	0.01
y12	1170.66	1170.66	0.00	1170.67	0.01
y11	1071.60	1071.58	−0.02	1071.60	0.00
y10	1000.56	1000.55	−0.01	1000.56	0.00
y9	887.47	887.47	0.00	887.50	0.03
y8	774.39	774.38	−0.01	774.39	0.00
y7	703.35	703.35	0.00	703.36	0.01
y6	646.33	646.33	0.00	646.33	0.00
y5	589.31	589.31	0.00	589.32	0.01
b ions					
b11	1205.52	1205.52	0.00	1175.54	−29.98
b12	1318.60	1318.57	−0.03	1288.61	−29.99
b16	1640.74	1640.70	−0.04	1610.80	−29.94
b17	1741.79	1741.79	0.00	1711.80	−29.99
b18	1888.86	1888.80	−0.06	1858.88	−29.98
b19	1945.88	1945.85	−0.03	1915.91	−29.97
b20	2073.97	2073.99	0.02	2044.01	−29.96

Finally, comparison with the much weaker ribosome-binding region upstream of the codon for Met^1 suggests that Met^{21} may be the preferred start site for translation of the BpKatG mRNA in *E. coli*.

Identification of the N Terminus of BpKatG—The N-terminal 34 residues predicted by the DNA sequence were not evident in the electron density maps of BpKatG (7), raising the question of whether they were present and disordered or absent as a result of N-terminal processing. The tryptic fragments corresponding to residues 1–9 and 19–26, including possible partial digest fragments, are absent from the spectrum, whereas the fragment corresponding to residues 27–40 is present, and its sequence is corroborated by MS/MS analysis (Table II). From these data, it can be concluded that the N-terminal sequence is truncated between residues 19 and 26, and this was confirmed by N-terminal sequencing to be at ^{22}SNEA. Truncation to Ser^{22} could have resulted from post-translational proteolysis or from translation initiation at Met^{21} followed by removal of the terminal formylmethionine. There is a strong Shine-Dalgarno sequence AGGAG upstream of the ATG codon for Met^{21}, and comparison with the much weaker ribosome-binding region upstream of the codon for Met^1 suggests that Met^{21} may be the preferred start site for translation of the BpKatG mRNA in *E. coli*.

TABLE V
Observed and expected mono-isotopic M + H⁺ masses of ions from the tryptic digest of HP1 and its W105F variant

Expected ion (*m/z*)	Observed in BpKatG	Observed in W105F	Peptide	Sequence	Confirmed by MS/MS
1110.52	No	1110.51	103–112	MAFHGAGTYR	Yes
1149.53	1149.52	No	103–112	MAWHGAGTYR	Yes
2534.20	2534.20	2534.20	247–271	ATFGNMGMNDEETVALIAGGHTLGK	Yes
3204.60	3204.60	3204.60	215–246	ACLGATEMGLIYVNPEGPDHSGEPLSAAAAIR	Yes
	3220.60	3220.58		Possible oxidation product of 215-246	No
4351.11	4352[a]	No		Trp-Tyr adduct of 103-112 and 215-246	No
	4383[a]	No		Two oxidations Trp-Tyr adduct	No
	4399[a]	No		Three oxidations and/or CH_3-S added to Trp-Tyr adduct	Yes
	4415[a]	No		Mixed ion of oxidized and modified Trp-Tyr adduct	No
	4431[a]	No		Mixed ion of oxidized and modified Trp-Tyr adduct	No

[a] Average mass of the cluster is presented. Difficulty in identifying the real monoisotopic ion in a mixture of ions precludes the accurate measurement of masses. The identification of oxidized forms of the fragments is complicated by the fact that every ion produces two daughter ions, from loss of water (−18) and loss of NH_3 (−17), giving rise to three overlapping series of ions differing by +16, −17, and −18. The situation is further complicated by the possibility that CH_3-S may also be present, producing a +46 series.

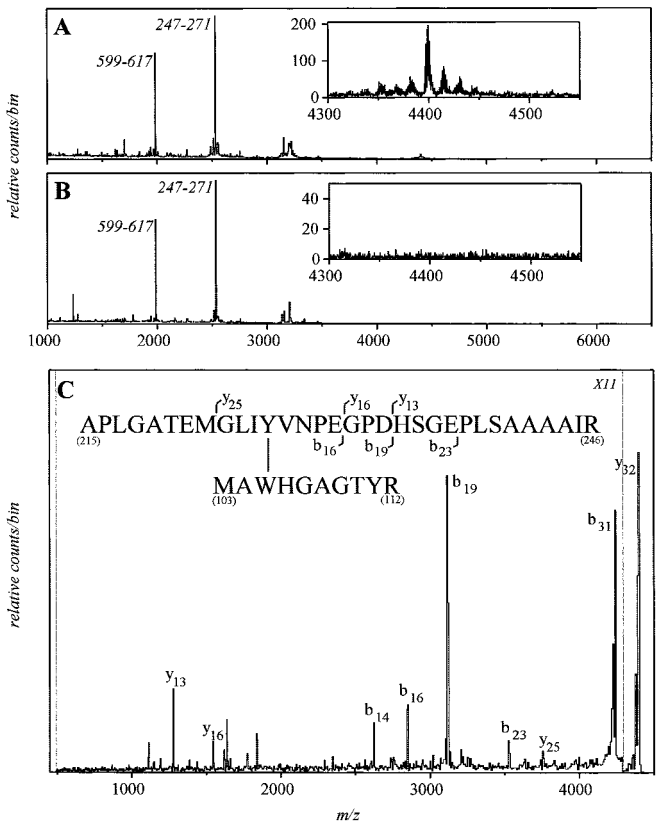

FIG. 6. **MALDI spectra of comparable HPLC fractions from tryptic digests of native HPI and the W105F variant.** *A*, the spectrum of HPLC fraction 20 of the digest of native HPI contains a cluster of ions (expanded in *inset*) formed by covalent linkage between Trp^{105} and Tyr^{226}. There were no measurable ions at higher *m/z*. *B*, the spectrum of HPLC fraction 21 of the W105F variant contains no measurable ions in the region from *m/z* 4300–4500. *C*, partial MS/MS analysis of the ion at *m/z* 4396 from *A*. The locations of the cleavage sites giving rise to the various ions are shown by *vertical lines*, and the ion designations are above or below the sequence. The ions y32 and y25 and all of the b series ions are 45 Da larger than expected from the sequence, and the ions y13 and y15 ions agree well with the expected sizes. The sizes of the ions are summarized in Table VI.

TABLE VI
Comparison of expected and observed mono-isotopic M + H⁺ masses of ions in the MS/MS spectrum shown in Fig. 6C

N	Expected ion	Observed ion	Difference
y ions			
y32	4351.11	4397.07	45.96
y25	3711.79	3757.75	45.96
y16	1548.78	1548.75	−0.03
y13	1279.68	1279.65	−0.03
b ions			
b14	2577.25	2623.27	46.02
b16	2803.34	2849.33	45.99
b19	3072.44	3118.37	45.93
b23	3482.60	3528.42	45.82
b31	4177.00	4222.77	45.77
b32	4333.10	4378.96	45.86

DISCUSSION

Mass spectrometry evidence for the Trp^{111}-Tyr^{238}-Met^{264} adduct in the tryptic digests of BpKatG corroborates the conclusions drawn from electron density maps. Large ions consistent with three peptides linked by Trp^{111}-Tyr^{238}-Met^{264} and two peptides linked by Trp^{111}-Tyr^{238} are evident in the spectrum of BpKatG but not in the spectrum of the W111F variant. The covalent bonds in the adduct are sensitive to breakdown under mass spectrometry conditions with the Tyr-Met bond being more labile, presenting indirect evidence for its existence in the breakdown products, including CH_3-S attached to Tyr^{238} and homoserine. In fact, the existence of ions differing only in having methionine or homoserine suggests that the breakdown of the Tyr-Met link may proceed by more than one pathway. The complete absence of any Trp^{111}-containing peptide indicates that breakdown of the Trp-Tyr bond, although less prevalent, produces a Trp-containing breakdown product that has not been identified. The tryptic digest of HPI presents direct evidence for the Trp-Tyr linkage and indirect evidence for the Tyr-Met linkage.

The core structure of the individual N- and C-terminal domains of catalase-peroxidases is very similar to the core structure of plant peroxidases, suggesting that the enzyme is a peroxidase that has adopted an efficient catalatic activity during evolution. A small number of clues for how this adaptation took place are provided by the structure of the active site. The active site Trp^{111} is clearly not required for the generation of compound I (Enz (Por-Fe^{III}) + H_2O_2 → Cpd I ($Por^{+\cdot}$-Fe^{IV} = O) + H_2O), which is unaffected by removal of the indole ring, but is required for the second stage reduction of compound I (Cpd I ($Por^{+\cdot}$-Fe^{IV} = O) + H_2O_2 → Enz (Por-Fe^{III}) + H_2O + O_2), which is reduced to 1% of native levels by removal of the indole ring. However, the distal Trp is not the sole determinant, because peroxidases with Trp in the equivalent position, such as cytochrome *c* peroxidase and ascorbate peroxidase, do not exhibit significant catalatic activity. Furthermore, the two other key active site residues in peroxidases, the arginine and histidine equivalent to Arg^{108} and His^{112} of BpKatG, are spatially oriented much the same as in BpKatG. Indeed, the root mean square deviation of the Cα of 133 residues in conserved α-helical segments, including the three active site residues, is just 0.97 Å comparing BpKatG and cytochrome *c* peroxidase (7).

The most significant differences between the catalase-peroxidases and the peroxidases, aside from sheer size, lie in the unusual post-translational modifications in the catalase-peroxidases, the Trp-Tyr-Met adduct, and the modified heme, and it is reasonable to consider how these features might make the catalase reaction possible.

The covalently linked residues would form a very rigid structure that would fix the position of the indole nitrogen of the essential Trp relative to the heme iron and imidazole ring of the essential His. Such precise positioning with no possibility of movement may be necessary to generate optimal interaction distances with the H_2O_2 for the reduction of compound I. Indeed, mutation of Met^{264}, which would prevent formation of at least part and possibly all of the covalent structure, significantly reduces catalatic activity, with little effect on peroxidatic activity (Table I), and mutation of the equivalent of Tyr^{238} in *Synechocystis* KatG has a similar effect (20). The covalent linkages may also affect the electronic environment of the indole, enhancing its ability to bind H_2O_2 for compound I reduction. In addition the adduct creates an obvious route for delocalization of the radical from the heme of compound I, a process recently demonstrated in *M. tuberculosis* KatG (21). From the standpoint of the peroxidatic reaction, electron tunneling from a peroxidatic substrate on the surface (7) to the heme for reduction of compound I or compound II may also be facilitated by the adduct.

A number of tryptic fragments, in particular those near the catalytic center, were present as clusters of ions differing by ~16 Da. This is suggestive of multiple oxidations, but the multiplicity of peaks poses a problem for this simple interpretation. The spectrum of the cluster of ions at *m/z* 4525 contains seven ions, although there are only three obvious sites of oxidation in the fragment, Trp^{111}, Met^{109}, and Met^{234}. Even allowing for up to two oxygens on each Met and one on the Trp, only five ions should be present. Furthermore, the only site of oxidation that was obvious in the electron density maps was the indole ring of Trp^{111} (7), and any other oxidations must be randomly distributed at an occupancy too low to be clearly evident. This makes it very likely that the additional, more intense ions, 46 Da and larger than the base ion, contain the CH_3-S portion of Met^{264} transferred to Tyr^{238}. Thus, at least two overlapping series of ions are responsible for the cluster at *m/z* ~4525.

It is tempting to speculate about the reaction mechanism responsible for the Trp-Tyr-Met covalent structure, and both free radical and ionic mechanisms can be presented that may be initiated by oxidation of the most reactive group, Met^{264}. However, structural analysis of variants lacking the three involved residues and other nearby residues are required to determine what residues are necessary and to see whether partial adducts can be formed will provide a much firmer basis for such speculation.

Acknowledgments—The cooperation of Dr. K. G. Standing and W. Ens in arranging use of the mass spectrometers in the TOF Laboratory of the Department of Physics at the University of Manitoba is appreciated.

REFERENCES

1. Heym, B., Alzari, P. M., Honoré, N., and Cole, S. T. (1995) *Mol. Microbiol.* **15,** 235–245
2. Welinder, K. G. (1991) *Biochim. Biophys. Acta* **1080,** 215–220
3. Hillar, A., Peters, B., Pauls, R., Loboda, A., Zhang, H., Mauk, A. G., and Loewen, P. C. (2000) *Biochemistry* **39,** 5868–5875
4. Regelsberger, G., Jakopitsch, C., Ruker, F., Krois, D., Peschek, G. A., and Obinger, C. (2000) *J. Biol. Chem.* **275,** 22854–22861
5. Regelsberger, G., Jakopitsch, C., Furtmuller, P. G., Rueker, F., Switala, J., Loewen, P. C., and Obinger, C. (2001) *Biochem. Soc. Trans.* **29,** 99–105
6. Yamada, Y., Fujiwara, T., Sato, T., Igarashi, N., and Tanaka, N. (2002) *Nat. Struct. Biol.* **9,** 691–695
7. Carpena, X., Lopraesert, S., Mongkolsuk, S., Switala, J., Loewen, P. C., and Fita, I. (2003) *J. Mol. Biol.* **327,** 475–489
8. Loewen, P. C., Switala, J., Smolenski, M., and Triggs-Raine, B. L. (1990) *Biochem. Cell Biol.* **68,** 1037–1044
9. Mead, D. A, Skorupa, E, S., and Kemper, B. (1985) *Nucleic Acids Res.* **13,** 1103–1118
10. Yanisch-Perron, C., Vietra, J., and Messing, J. (1985) *Gene* (*Amst.*) **33,** 103–119
11. Kunkel, T. A., Roberts, J. D., and Zakour, R. A. (1987) *Methods Enzymol.* **154,** 367–382
12. Sanger, F. S., Nicklen, S., and Coulsen, A. R. (1977) *Proc. Natl. Acad. Sci. U. S. A.* **74,** 5463–5467
13. Rørth, M., and Jensen, P. K (1967) *Biochim. Biophys. Acta* **139,** 171–173
14. Layne, E. (1957) *Methods Enzymol.* **3,** 447–454
15. Smith, A. T., Santana, N., Dacey, S., Edwards, M., Bray, R. C., and Thorneley, R. N. (1990) *J. Biol. Chem.* **265,** 13335–13343
16. Krutchinsky, A. N., Chernushevich, I. V., Spicer, V. L., Ens, W., and Standing, K. G. (1998) *J. Am. Soc. Mass Spectrom.* **9,** 569–579
17. Verentchikov, A. N., Ens, W., and Standing, K. G. (1994) *Anal. Chem.* **66,** 126–133
18. Loboda, A. V., Krutchinsky, A. N., Bromirski, M., Ens, W., and Standing, K. G. (2000) *Rapid Commun. Mass Spectrom.* **14,** 1047–1057
19. Evans, S. (1993) *J. Mol. Graphics.* **11,** 134–138
20. Jakopitsch, C., Auer, M., Ivancich, A., Rüker, F., Furtmüller, P. G., and Obinger, C. (2003) *J. Biol. Chem.* **278,** 20185–20191
21. Chouchane, S., Girotto, S., Yu, S., and Magliozzo, R. S., (2002) *J. Biol. Chem.* **277,** 42633–42638